Effects of Axial Coordination on Immobilized Mn(Salen) Catalysts.

ARTICLE *in* THE JOURNAL OF PHYSICAL CHEMISTRY A · OCTOBER 2014

Impact Factor: 2.69 · DOI: 10.1021/jp506206b · Source: PubMed

5 AUTHORS, INCLUDING:

Ricardo Mosquera

University of Vigo

144 PUBLICATIONS **1,814** CITATIONS

SEE PROFILE

André Melo

University of Porto

55 PUBLICATIONS **386** CITATIONS

SEE PROFILE

Cristina Freire

University of Porto

230 PUBLICATIONS **3,194** CITATIONS

SEE PROFILE

Natália D. S. Cordeiro

University of Porto

245 PUBLICATIONS **3,049** CITATIONS

SEE PROFILE

THE JOURNAL OF PHYSICAL CHEMISTRY A

Article

pubs.acs.org/JPCA

Effects of Axial Coordination on Immobilized Mn(salen) Catalysts

Filipe Teixeira,*[,†] Ricardo A. Mosquera,[‡] André Melo,[†] Cristina Freire,[†] and M. Natália D. S. Cordeiro*[,†]

[†]REQUIMTE, Departamento de Química e Bioquímica, Faculdade de Ciências, Universidade do Porto, Rua do Campo Alegre, 4169-007 Porto, Portugal

[‡]Departamento de Química Física, Facultade de Química, Universidade de Vigo, 36310 Vigo, Galicia, Spain

Supporting Information

ABSTRACT: The consequences of anchoring Mn(salen) catalysts onto a supporting material using one of the vacant positions of the metal center are tackled by studying several Mn(salen) complexes with different axial ligands attached. This is accomplished using Density Functional Theory at the X3LYP/Triple-ζ level of theory and the Atom In Molecules formalism. The results suggest that both Mn(salen) complexes and their oxo derivatives should lie in a triplet ground state. Also, the choice of the axial ligand bears a moderate effect on the energy involved in the oxidation of the former to oxo-Mn(salen) complexes, as well as in the stability of such complexes toward ligand removal by HCl. AIM analysis further suggests that the salen ligand acts as a "charge reservoir" for the metal center, with strong correlations being obtained between the charge of salen and the electron population donated by the axial ligand to the metal center. Moreover, the results suggest that the Mn atom in Mn(salen) complexes holds different hybridization of its valence orbitals depending on the type of axial ligand present in the system.

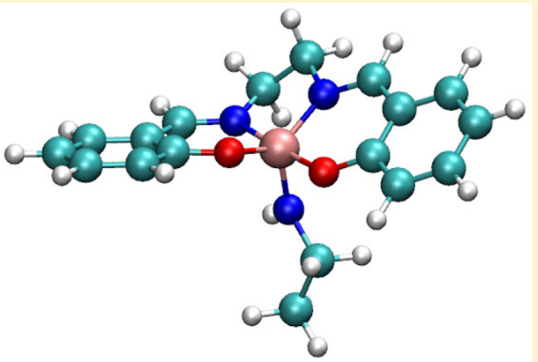

INTRODUCTION

Manganese−salen complexes, hereafter Mn(salen), have long been known to efficiently catalyze the epoxidation of unfunctionalized alkenes. Chiral variations on this scaffold attain remarkable enantioselectivity upon the epoxidation of olefins.[1−3] Being so, the immobilization of Mn(salen) complexes onto a supporting material has yielded an assortment of novel materials with interesting catalytic properties.[4,5] Among the different immobilization strategies that have came to light in recent years, one of the most common is covalent attachment of the metal center onto a functionalized supporting material (see Figure 1). The functional group at the surface of the supporting material acts as a donor ligand to the manganese atom. Such donor ligands usually occupy one of the axial positions of the coordination sphere of manganese, with the salen ligand lying in a quasi-planar conformation and binding to the four equatorial sites of the metal center.[6,7] The use of axial coordination as an immobilization strategy raises interesting questions on how it may affect the electronic structure of the catalyst and moreover, whether it is responsible for altering its catalytic efficiency or chemoselectivity.

Early experimental studies in homogeneous media show that the presence of nitrogen heterocycle additives such as pyridine *N*-oxides, pyridines, or imidazoles bear a strong influence over the rate, yield, and selectivity of Mn(salen) catalysts. It was postulated by Kochi that such bases act as donor ligands at the axial position. This would stabilize the active oxo-Mn(salen) species formed in the course of the catalytic cycle, thus increasing the rate and yield of the reaction.[2,7,8]

This subject has also been tackled from the theoretical point of view, with early studies showing that the omission of chloride from the axial position of the Mn(salen) model would make it conform poorly to the experimental evidence.[9,10] Moreover, Cavallo and Jacobsen reported that a hypochloride anion coordinated to the axial position of the manganese atom would facilitate the regeneration of the active oxo-Mn(salen) species in a biphasic H_2O/CH_2Cl_2 system.[11] However, a general theoretical model for explaining the effect of axial donor ligands on the catalytic properties of Mn(salen) complexes has eluded later efforts by Cavallo and Jacobsen.[12] The use of a truncated Mn(acacen') model as a surrogate for a proper Mn(salen) complex has been suggested as a possible explanation for such failure.[7,13,14] Thus, despite the wealth of information availabe on the structure and reactivity of chlorinated Mn(salen) systems,[3,8,9,14−20] the study of their immobilized counterparts is mainly restricted to the experimental exploration of novel immobilization schemes.[21−29] The development of novel hybrid nanocatalysts though axial immobilization and the increasing demand of such materials in the pursue of novel synthetic strategies entices this question to be addressed once again.

Despite its limitations, Density Functional Theory (DFT) may be an useful tool for obtaining the electron density of these transition metal complexes. It is known that the electron density that results from DFT calculations is comparable to that

Received: June 22, 2014
Revised: October 5, 2014

   dx.doi.org/10.1021/jp506206b | J. Phys. Chem. A XXXX, XXX, XXX−XXX

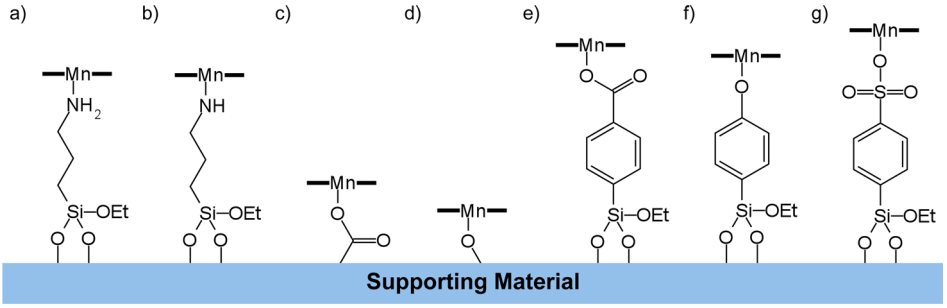

Figure 1. Examples of covalent attachment of Mn(salen) complexes onto a supporting material: (a) and (b) using ATPES as a linker molecule; (c) and (d) covalent attachment to hydroxyl and carboxyl functionalized carbon materials; (e), (f), and (g) using phenoxy, phenylbarboxyl, or phenylsulfide linkers. The salen ligand in these schemes is represented in a simplified manner by the two bold lines around the manganese atom.

of high level wave function methods, given a basis set with enough flexibility. This is possible because the shape and spread of the Kohn–Sham orbitals is a function of the electron density, that includes the effect of electron correlation.[30,31] The topology of the electron density can be analyzed under the formalism of Bader's theory of Atoms in Molecules (AIM). This analysis allows the establishment of effective atomic charges and spin densities, which provide means to rationalize the properties and chemical reactivity of these compounds.[32,33] Although AIM may exaggerate the charge separation between bonded atoms, these somewhat exaggerated charges provide a "high contrast" picture of the charge distribution along the system, when compared with more traditional population analysis methods, as recently reported by Teixeira et al.[34] Moreover, the analysis of the Laplacian of the electron density provides an useful tool for the localization of regions in which the electron density is locally concentrated. Such regions are traditionally related to the presence of localized orbitals, nonbonding electron pairs, and unpaired electrons.[35]

In this work, the effect of immobilization of Mn(salen) complexes through axial coordination is studied. This is done using two complementary points of view: in one hand, energy differences for some typical reactions, obtained from first-principles DFT calculations, are compared. However, the topology of the electron density of the complexes in question is surveyed under the AIM formalism. An assortment of possible axial ligands was selected, as shown in Figure 2. These ligands attempt to mimic the local chemical environment of the metal center in some successful anchoring strategies,[22,25,36−38] with chloride-coordinated complexes **1-re** and **1-ox** being used as reference. The results are given in the hope of providing a model for the effect of axial coordination to Mn(salen) catalysts.

■ COMPUTATIONAL METHODS

Throughout this work, we use the nomenclature established in Figure 2, in which the number of the compound is determined by the axial ligand used and the oxidation state of the metal center is given by an appropriate suffix (**re** and **ox** for Mn^{III}(salen) and oxo-Mn^{V}(salen) complexes, respectively). Moreover, this work follows the nomenclature used by Cavallo and Jacobsen,[39] in which the relevant electronic states are identified by a notation indicating the respective total spin density $S = |\rho_\alpha(\mathbf{r}) - \rho_\beta(\mathbf{r})|$. So that the symbols *S0*, *S2*, and *S4* refer to total spin densities of zero (singlet), two (triplet), and four (quintet) unpaired electrons, respectively. When needed, these symbols will be used as suffixes when referring to a particular state of a given compound.

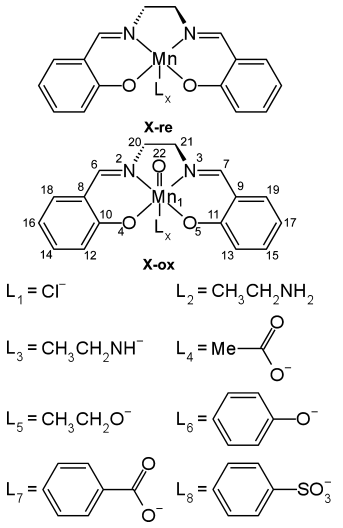

Figure 2. Generic structural formula of Mn(salen) (**X-re**) and oxo-Mn(salen) (**X-ox**) complexes, with different axial ligands.

DFT calculations were performed using the Orca program package, version 2.8.[40] The X3LYP functional was chosen for all DFT calculations based on its reported accuracy when dealing with transition metal complexes[41,42] and also our previous experience with its application in the study of Mn(salen) complexes.[14,34] A mixed basis set was used in this work, which is available in the software under the keyword DefBas-4. This corresponds to a triple-ζ valence (TZV) basis set with contraction pattern {311/1} for hydrogen, {62111/411/11} for other atoms in the main group and {842111/63111/411/1} for manganese.[43,44]

The geometry of the 16 Mn(salen) systems were optimized at their *S0*, *S2*, and *S4* states. For the *S2* and *S4* states, all calculations were performed under an unrestricted Kohn–Sham (KS) scheme, with independent treatment of the electron densities $\rho_\alpha(\mathbf{r})$ and $\rho_\beta(\mathbf{r})$. In their turn, *S0* systems were treated under a restricted KS, following the results of preliminary calculations that validate the use of such formalism.[34] Following the method established by Cavallo and Jacobsen,[45] the folding of the salen ligand was evaluated by means of the ligand bent angles, ϕ_e and ϕ_u, as well as the pyramidalization distance (d_p). A bent angle, ϕ, is defined as $\phi = 180° - \angle(X_{NN} - Mn - X_{NO})$ where X_{NN} and X_{NO} refer to the midpoint between the two nitrogen atoms and the midpoint between adjacent N,O atoms, respectively. Following the numbering scheme shown in Figure 2, the adjacent N,O atoms considered in ϕ_e are $N_{(2)}$ and $O_{(4)}$, whereas ϕ_u refers to atoms $N_{(3)}$ and $O_{(5)}$.

dx.doi.org/10.1021/jp506206b | J. Phys. Chem. A XXXX, XXX, XXX−XXX

The nuclear Hessian of each system at the equilibrium geometry was calculated at the same level of theory as the geometry optimization, and the subsequent vibrational analysis allowed the confirmation of the equilibrium geometries as true minima in the potential energy surface. The results from these calculations further allowed for zero-point vibrational corrections and other thermochemistry parameters to be estimated for these systems.

A conversion utility (Molden2AIM, from Prof. Wenli Zou at the Southern Methodist University, Dallas[46]) was used to convert the output of Orca into a suitable format for the AIM analysis software. The topology of the electron density ($\rho(\mathbf{r})$) was surveyed using the AIMALL program package,[47] which was also used for the integration of the atomic basins and determination of effective atomic charges, spin densities and related properties. The topology of the Laplacian of the electron density, $\nabla^2\rho(\mathbf{r})$, was surveyed using Bader's AIMPAC program suite.[48] Following the convention used by several authors, the $L(\mathbf{r})$ function will be defined as $-1/4\nabla^2\rho(\mathbf{r})$, for which a local maximum corresponds to a local concentration of the charge density, usually interpreted as the localization of a lone electron or nonbonding pair of electrons.[35,49]

All statistical analysis were carried out using the R language and software package.[50] In all cases, distances were expressed in angstroms, angles in degrees, and charges and charge densities in atomic units.

RESULTS AND DISCUSSION

The geometry of the different complexes was successfully optimized. As expected, the salen ligand assumes a quasi-planar conformation at the equilibrium geometry, as exemplified in Figure 3. Despite this, the pyramidalization distance, d_P, varies

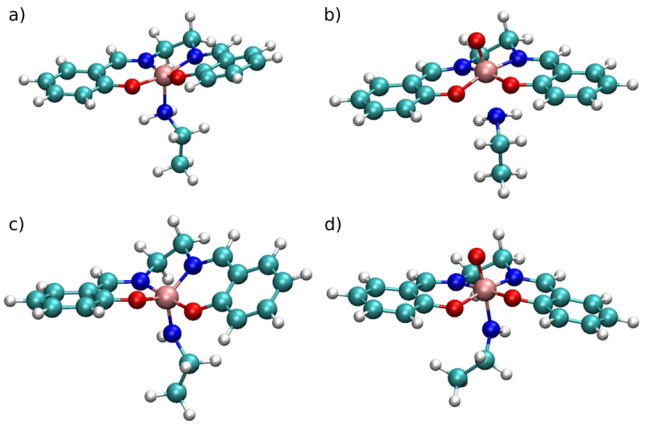

Figure 3. Equilibrium geometries of 2-re (a), 2-ox (b), 3-re (c), and 3-ox (d) at the *S2* state, obtained at the X3LYP/DefBas-3 level of theory.

significantly with respect to the choice of axial ligand, with average values of 0.32 ± 0.12 A and 0.17 ± 0.05 A for Mn(salen) and oxo-Mn(salen) species, respectively. However, ϕ_e and ϕ_u show limited variability, with average values of 169 ± 4° and 168 ± 6°, respectively, in Mn(salen) complexes, and 160 ± 8° and 167 ± 5°, respectively, in oxo-Mn(salen) complexes. These results show that the salen ligand sits in a slightly bent conformation, in good accordance to previous works.[6,12]

Relative Energies of *S0*, *S2*, and *S4* States. Three spin states (*S0*, *S2*, and *S4*) are conceivable for Mn(salen) and oxo-Mn(salen) complexes. The relative energies of the *S2* and *S4* states of each complexes (taking *S0* as reference) are given in Table 1. The results suggest that the ground state of Mn(salen) species may be either *S0* or *S2*, depending on the axial ligand.

Table 1. Energies of *S2* and *S4*, Relative to *S0*, for the Mn(salen) and oxo-Mn(salen) Complexes with Different Axial Ligands[a]

	Re		Ox	
X	*S2*	*S4*	*S2*	*S4*
1	−14.1	26.9	−10.9	212.2
2	0.6	27.6	−12.8	212.8
3	1.9	67.3	−12.8	156.4
4	−7.7	37.2	−9.0	213.5
5	−2.6	44.9	−4.5	219.9
6	−21.8	26.3	−2.6	159.0
7	−14.7	32.1	−9.6	214.1
8	−12.8	23.7	−11.5	217.9

[a]All values are given in kJ · mol^{-1} and include zero-point vibrational corrections.

In the homogeneous phase, **1-re** is likely to have an *S2* ground state, in accordance with the experimental evidence,[15,51,52] and also with high level quantum mechanics calculations using triple-ζ basis sets.[6,53] However, the *S0* and *S2* states of **2-re**, **3-re**, and **5-re** are quasi-degenerate. Within the accuracy of DFT, it is difficult to predict which of *S0* or *S2* is the ground state for these complexes without further considerations. In their turn, oxo-Mn(salen) species show a clear tendency toward an *S2* ground state with a low lying *S0* excited state. In all cases, it is unlikely that any of the complexes would adopt *S4* as their ground state. Axial coordination with $PhCOO^-$ or $PhSO_3^-$ appears to have the least impact on the ordering and relative energies of the *S0*, *S2*, and *S4* states. However, the most noticeable deviations to the overall behavior (in terms of ordering and energetic differences between spin states) are observed for species **3-re** and **3-ox**, as shown in Table 1.

The results from vibrational analysis show that zero-point corrections bear little effect on the overall ordering and energy differences between spin states. The same also applies to the enthalpic corrections at 298.15 K. However, an analysis of the relative Gibbs energies reveals a strong preference of the *S2* state for all complexes, the electronic component of the entropy, S_{el} playing a major role in the stabilization of *S2* with respect to *S0*. At 298.15 K, the energetic contributions of S_{el} are 2.72 kJ mol^{-1} and 3.99 kJ mol^{-1} for complexes at the *S2* and *S4* state, respectively, thus pushing the *S2* state bellow *S0* for all cases under consideration. Despite the approximations involved in DFT, these results are significant, as they support the reaction models that predict the catalytic cycle of Mn(salen) complexes to occur exclusively in the *S2* state.[6,11,13,54] The absolute energies, zero-point vibrational energy, and total entropy and Gibbs energy corrections at 298.15 K are given in the Supporting Information (SI).

Reaction Energetics. An estimate of the energy involved in the oxidation of Mn(salen) complexes to their oxo-Mn(salen) analogues, ΔE_{ox}, was made by considering the energy balance of this reaction using H_2O_2 as oxidant and water as its byproduct. This procedure further assumed spin conservation during the oxidation process, and the results are displayed in Table 2. The oxidation process is strongly exoenergetic and the value of ΔE_{ox} for the homogeneous catalyst appears to be close to the average of all other cases studied, at all spin states. Considering the *S2* case in more detail, ΔE_{ox} is greater (in

dx.doi.org/10.1021/jp506206b | J. Phys. Chem. A XXXX, XXX, XXX−XXX

Table 2. Energy Balance for the Oxidation of Mn(salen) to Their oxo-Mn(salen) Analogues, ΔE_{ox}, Using H_2O_2 as Oxidant, With Different Axial Ligands, and at Different Spin States[a]

X	S0	S2	S4
1	−529.3	−526.1	−344.1
2	−539.0	−552.4	−353.7
3	−426.1	−440.9	−337.0
4	−522.9	−524.2	−346.7
5	−506.3	−508.2	−331.3
6	−536.4	−517.2	−403.7
7	−529.3	−524.2	−347.3
8	−549.9	−548.6	−355.6

[a]All values are given in kJ·mol^{-1} and include zero-point vibrational corrections.

absolute value) for the oxidation of **8-re**, and smaller for **3-re**, with a range of about 100 kJ mol^{-1} between these two cases. The results suggest that coordination with Et-NH-yields the less stable oxo-derivative, relative to its parent complex.

A second type of energy balance, ΔE_{lx}, was considered in which the axial ligand is removed by HCl, yielding the conjugate acid of the original axial ligand and the corresponding complex **1-re** or **1-ox**. This reaction is of some importance as it allows some sense on the spontaneousness of catalyst leaching processes. As shown in Table 3, compounds with different axial ligands behave rather differently. Focusing on the *S2* state, and assuming spin conservation, the ligand displacement reaction is always energetically unfavored for complexes coordinated with L_2 and L_5. By contrast, the displacement of a carboxilate group in the axial position of the manganese atom (L_4 and L_7) is energetically favored. However, the remaining cases shown in Table 3 not only reveal that the oxidation state of the metal center bears some influence on the energetic balance for this type of reaction, but also points toward the possibility that strong ligands are displaced from the oxo-complexes (**3-ox**) with a favorable energetic balance. Moreover, the results in Table 3 strongly suggest that the energetics of ligand exchange reactions within this set of compounds cannot be fully explained by the relative basicity of the axial ligand.

Table 3. Energy Balance for the Removal of the Axial Ligand of Mn(salen) and oxo-Mn(salen) Complexes Using HCl, ΔE_{lx}, at Different Spin States[a]

	Re			Ox		
X	S0	S2	S4	S0	S2	S4
1	0.0	0.0	0.0	0.0	0.0	0.0
2	102.6	87.9	102.0	112.2	114.1	111.6
3	72.2	56.2	31.8	−31.0	−29.0	24.8
4	−7.3	−13.7	−17.5	−13.7	−15.6	−14.9
5	38.5	26.9	20.5	15.4	9.0	7.7
6	0.3	8.0	1.0	7.4	−1.0	60.6
7	−10.4	−9.8	−15.5	−10.4	−11.7	−12.3
8	−2.0	−3.3	1.2	18.5	19.2	12.7

[a]All values are given in kJ·mol^{-1} and include zero-point vibrational corrections.

AIM Analysis. In order to further rationalize the observations described above, an AIM population analysis was made, the results of which are displayed in Figure 4. Our discussion of the AIM results will focus on the *S2* state, due to the likelihood of this being the ground state for all complexes. Moreover, the results from the AIM analysis for these compounds at their *S0* state are very similar to those shown here for the *S2* state, in accordance to previous work.[34]

As shown in Figure 4, the effective atomic charges of Mn and $O_{(22)}$ are very stable with respect to the different axial ligands tested, with average values of +2.69 ± 0.05 *e* and −0.89 ± 0.02 *e*, respectively in the oxo-Mn(salen) species. The effective charge of the metal center also shows little variation within the reduced Mn(salen) complexes, with an average value of +2.23 ± 0.13 *e*. However, the combined effective charges of the salen ligand, q_S, show significant variations with respect to the oxidation state of the metal center and also with respect to the choice of axial ligand. The coefficient of variation (CV) for q_S being 13.6% in the reduced Mn(salen) complexes and 8.1% in their oxo derivatives. The combined effective charges of the axial ligand, q_L, also present huge variations, with CV of 69.6% and 60.7% for the reduced and oxidized manganese complexes, respectively. Such results point to a very diverse behavior of the tested axial ligands, the consequences of which will be explored in the remainder of this work. For simplicity, the following discussion will refer to the amount of electrons transferred from salen, L_x and $O_{(22)}$ to the metal center; these quantities being referred to as e_S, e_L, and e_O, respectively. These quantities (shown in Table 4) were calculated assuming a −1 charge for the axial ligand (with exception of L_2, which is neutral in its free form), and a −2 charge of the free salen and oxo ligands.

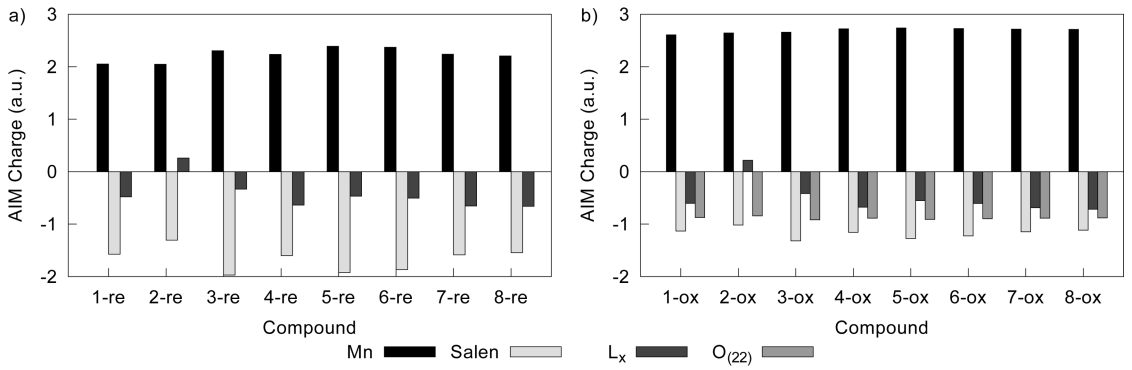

Figure 4. AIM charge distribution for the Mn(salen) (a) and oxo-Mn(salen) (b) complexes under study at their *S2* state at the X3LYP/DefBas-4 level of theory.

dx.doi.org/10.1021/jp506206b | J. Phys. Chem. A XXXX, XXX, XXX−XXX

Table 4. Transferred Electrons from Salen, e_S, the Axial Ligand, e_L, and $O_{(22)}$, e_O, to the Manganese Atom, at the *S2* State

	e_S		e_L		e_O
AxLig	Re	Ox	Re	Ox	Ox
1	0.428	0.868	0.520	0.397	1.127
2	0.694	0.983	0.260	0.218	1.158
3	0.028	0.682	0.666	0.583	1.082
4	0.401	0.844	0.363	0.323	1.113
5	0.079	0.726	0.532	0.449	1.089
6	0.133	0.776	0.496	0.394	1.102
7	0.415	0.853	0.348	0.314	1.114
8	0.455	0.886	0.339	0.284	1.120

Table 4 allows the ordering of the different ligands by their donor capability, with L_2 being the weakest donor, and L_3 the strongest one. The chloride anion, L_1, which is the axial ligand usually found in homogeneous media, falls halfway between the two most extreme cases under consideration, although with some offset toward the strongest donors. The values of e_L for the Mn(salen) and oxo-Mn(salen) species are strongly correlated (r^2 = 0.9615) showing that e_L is a good estimator for the donor power of the axial ligand in this collection of compounds, as shown in Figure 5a.

The amount of electron population transferred from the axial ligand to manganese is reduced to about 82% upon oxidation of the metal center, as shown in Figure 5a. This is in apparent contradiction with the common sense perspective according to which the electron depleted Mn^V atom should be able to withdraw more electron density from the axial ligand. However, further analysis of the data in Table 3 shows that the salen ligand is the main responsible for the seemingly stable charge of the manganese atom. This is notorious upon oxidation of the metal center, which is accompanied by a large increase in the charge transferred from salen to Mn. As shown in Figure 5b, the overall charge of the salen ligand is strongly correlated to the amount of charge transferred between the axial ligand and the metal center, this effect being more noticeable in the reduced Mn(salen) complexes than in their oxo-analogues.

The picture emerging from Table 4 and Figure 5 points to the fact that strong donor ligands in the axial position of Mn(salen) complexes increase the electron population in the salen ligand. This is well illustrated by the case of the neutral ligand L_2: the small amount of electron density it donates (less that 0.27 *e*) implies that a greater amount of negative charge must be transferred from the salen ligand to the manganese atom in **2-re** and **2-ox**. This concept of salen as a "charge reservoir" was described in a recent work that compares the charge distribution in $Mn(salen)^+$, Mn(salen)Cl, and their respective oxo-analogues.[34] The results in this work further suggest that this concept may be an important factor for the rationalization of the role of the axial ligand.

Within the salen ligand, an analysis of the effective atomic charges of its constituent atoms revealed that the $N_{(2,3)}$ and $O_{(4,5)}$ bear most of the ligand's negative charge (about −1.1 *e* per atom). The excess negative charge in these atoms is partly counterbalanced by the prominent positive charges of $C_{6,7}$ and $C_{10,11}$, as mentioned in the recent work by Teixeira et al.[34] The effective atomic charges of these four carbon atoms present the wider variation with respect to the different axial ligands. The combined charge of these four atoms (hereafter denoted q_C) behaves very differently according to the oxidation state of the metal center. In Mn(salen) complexes, q_C assumes a bimodal distribution, with values of about 1.60 *e* in **3-re**, **5-re**, and **6-re**; and 1.79 e for the remaining complexes. In the oxo-Mn(salen) species, **2-ox** stands as an exception, with an extremely low q_C (+1.94 *e* against an average value of +2.11 ± 0.07 *e*). Excluding **2-ox** reveals that q_C shows little variation in oxo-Mn(salen) complexes (with an average value of +2.133 ± 0.010 e). Contrary to previous reports on the charge distribution on other conjugated systems,[55,56] the changes in q_S are mainly due to the effective atomic charge of the carbon atoms, while the hydrogen atoms retain their charges relatively unaffected by the choice of axial ligand or the oxidation state of the metal center. Such observations suggest that the charge transfer mechanism from salen to Mn should occur through the ligand's conjugated π system, leaving the σ skeleton of the ligand relatively unaffected.

Further exploration of the data also shows that q_S, e_L, and the pyramidalization distance, d_P, are closely correlated in both reduced and oxidized species, as shown in Figure 6. The results in Figure 6a suggest that weak donor ligands may attach loosely to the manganese atom. For the reduced Mn(salen) complexes under such conditions, the coordination sphere of the metal center would resemble that of the four-coordinated Mn(salen)+

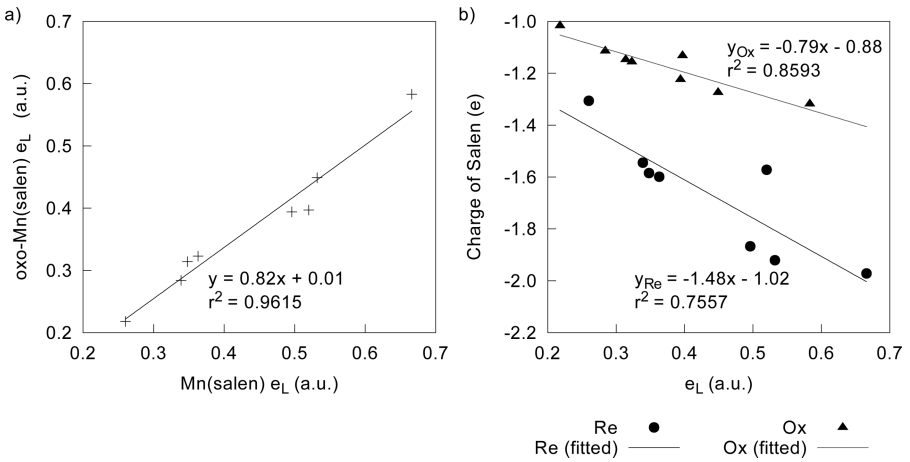

Figure 5. Relationship between the electronic population transferred from L_x to the metal center, e_L, in the reduced Mn(salen) complexes and their oxo derivatives (a) and charge of the salen ligand as a function of e_L (b).

dx.doi.org/10.1021/jp506206b | J. Phys. Chem. A XXXX, XXX, XXX−XXX

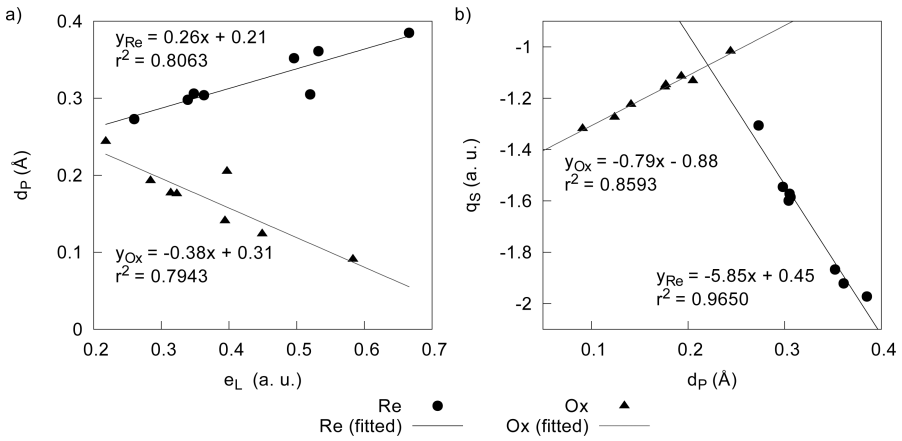

Figure 6. Pyramidalization distance, d_P, as a function of e_L (a), and the combined charge of the salen ligand, q_S, as a function of d_P (b) for Mn(salen), Re, and oxo-Mn(salen), Ox, complexes.

species,[34] in which the nitrogen and oxygen atoms of the salen ligands arrange in a nearly square planar geometry. With increased strengthening of the Mn—L_x bond, the geometry around the manganese atom rearranges to a trigonal bipyramidal molecular arrangement, thus increasing d_P. A similar reasoning justifies the rearrangement of oxo-Mn(salen) complexes from the near trigonal bipyramidal geometry found in oxo-Mn(salen)+ (which is only slightly distorted in the presence of weak donor ligands) to the near octahedral geometry attained around the metal center in the presence of strong donor ligands.[6,34] Also, Figure 6 suggests that the charge of the salen ligand is strongly influenced not only by the oxidation state of the manganese atom, but also by the charge donating ability of the axial ligand and by the conformation assumed by the salen ligand itself, this last factor being also moderately correlated to e_L. This suggests that both electronic and steric effects play a role in defining the role of the axial ligand.

At this point, an analysis of $L(\mathbf{r})$ in the vicinity of the manganese atom may shed some light on the relationship between charge transfer and the conformation of the salen ligand. For the sake of simplicity, this discussion will be done by comparing Mn(salen) complexes with L_2 and L_3, as they are the weakest and strongest donor ligand in this study, respectively. Figure 7 shows the spin density of compounds **2-re**, **2-ox**, **3-re**, and **3-ox** and the local maxima, (3,−3) critical points, of $L(\mathbf{r})$ in overlay. The results show that there is a correspondence between the center of the lobes of the spin density and the maxima of $L(\mathbf{r})$. In turn, these maxima bisect the angles formed between the bonds of Mn to the nitrogen and oxygen atoms of salen. In the case of **2-re** (Figure 7a), such configuration implies a sp^2d^2 hybridization scheme for Mn^{III} in which the five hybrid orbitals are responsible for the square pyramidal arrangement of the bonds around the metal center, two 3*d* orbitals are occupied by one electron each, and the remaining 3*d* orbital is empty. When using a stronger donor ligand (as in the case of **3-re**, Figure 7c), the localization of the maxima of $L(\mathbf{r})$ relative to the bonds around Mn is more compatible to what would be expected for an sp^3d hybridization of the metal center, which allows the two 3*d* orbitals to be occupied by only one electron each, leaving the two remaining 3*d* orbitals empty. In the oxo-Mn(salen) complexes, the sp^3d^2 hybridization is observed, warranting the near octahedral arrangement of the atoms bonded to the metal center and ensuring two of the remaining

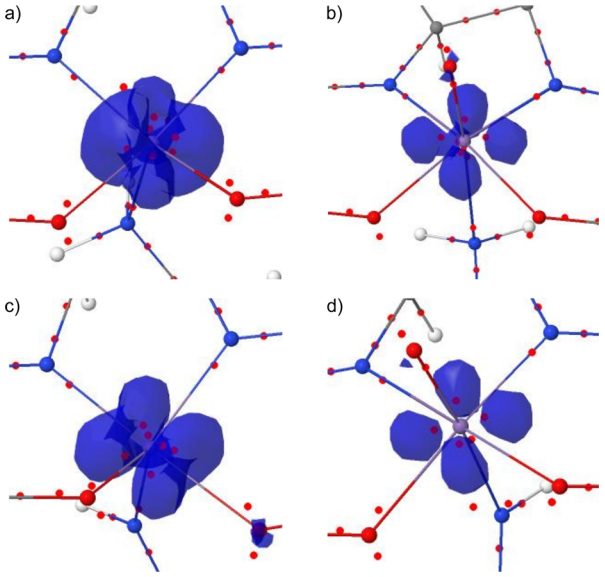

Figure 7. Depictions of the local maxima of $L(\mathbf{r})$ in the vicinity of the manganese atom, with the 0.05 isosurface of the spin density overlapped, for compounds: **2-re** (a), **2-ox** (b), **3-re** (c), and **3-ox** (d).

3*d* orbitals to be half filled. The fact that a change in the hybridization of Mn is observed in Mn(salen) complexes but not in their oxo derivatives conforms nicely with the less pronounced slope observed for the latter complexes in Figure 6b.

Finally, an interesting feature of the electronic structure of the oxo-Mn(salen) complexes under study was the dependence of the electron density at the bond critical point between the Mn and $O_{(22)}$ ($\rho_{BCP}(Mn{=}O_{(22)})$) and e_L, which is shown in Figure 8a. Although $\rho_{BCP}(Mn{=}O_{(22)})$ varies little within the cases under study (CV = 2.14%), its variation appears to be strongly influenced by e_L, as shown in Figure 8a. These results suggest a weaker $Mn{=}O_{(22)}$ bond for complexes with strong donors at their axial position. Such a fact may be also related to the relationship between d_P and ΔE_{ox}, which is depicted in Figure 8b (cf. Table 2). Contrary to what was postulated by Kochi,[2,7,8] strong donor ligans destabilize the oxo-Mn(salen) complexes, relative to their reduced parent compounds, as illustrated in Figure 7b. More importantly, the results show that a minute modification on the electron distribution on these

dx.doi.org/10.1021/jp506206b | J. Phys. Chem. A XXXX, XXX, XXX−XXX

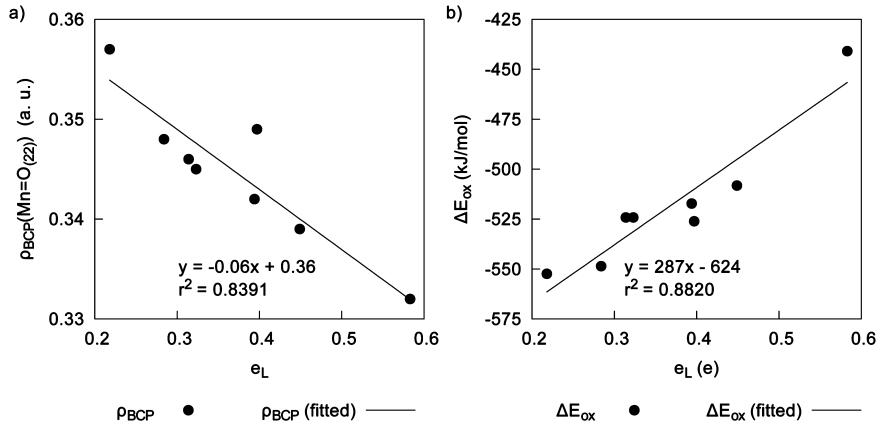

Figure 8. Electron density at the bond critical point between the Mn and $O_{(22)}$, $\rho_{BCP}(Mn—O_{(22)})$ as a function of e_L (a); and the energy involved in the formation of oxo-Mn(salen) complexes from Mn(salen) and H_2O_2, ΔE_{ox} as a function of e_L in the oxo-Mn(salen) species (b).

systems may have a strong impact on the energy balance of the reactions in which these compounds take part.

CONCLUSIONS

In this work, several Mn(salen) and oxo-Mn(salen) complexes were studied in order to probe the effect that different axial ligands may have in the structure and reactivity of these complexes. The results show that the axial ligand influences the energy balance of the oxidation of Mn(salen) complexes to their oxo-Mn(salen) counterparts, with strong donor ligands yielding the less stable oxo-Mn(salen) complexes. Also, the charge of the salen ligand is strongly correlated to the donating power of the axial ligand, while the charge of Mn and of the oxo ligand (when present) remain stable. This constitutes further evidence that the salen ligand acts as a "charge reservoir" for the Mn atom (or the Mn═O group in oxo-Mn(salen) complexes). In general, the reduced Mn(salen) complexes are more sensitive to the choice of axial ligand than their oxo derivatives. In both cases weak donor ligands result in a diminished electron population of the salen ligand, and vice versa. In the case of Mn(salen) complexes, AIM analysis shows that the axial ligand also affects the hybridization of the metal center.

The results presented here show that a broad range of chemical properties are affected by changing the axial ligand in Mn(salen) complexes and their derivatives. Such variations suggest that, when dealing with immobilization of Mn(salen)-type catalysts, the issue of choosing the linker molecule strongly affects the chemical properties of the immobilized catalyst.

ASSOCIATED CONTENT

Supporting Information

Equilibrium geometries of relevant species and reaction energetics data. This material is available free of charge via the Internet at http://pubs.acs.org.

AUTHOR INFORMATION

Corresponding Authors

*E-mail: filipe.teixeira@fc.up.pt.
*E-mail: ncordeir@fc.up.pt.

Notes

The authors declare no competing financial interest.

ACKNOWLEDGMENTS

This work has been supported by Fundação para a Ciência e Tecnologia (FCT) through Grant No. PEst-C/EQB/LA0006/2013 and Project NORTE-07-0124-FEDER-000067—NANOCHEMISTRY. F.T. further acknowledges FCT for a doctoral Grant (SFRH/BD/64314/2009).

REFERENCES

(1) Katsuki, T. Mn-salen Catalyst, Competitor of Enzymes, for Asymmetric Epoxidation. *J. Mol. Catal. A: Chem.* **1996**, *113*, 87−107.
(2) McGarrigle, E. M.; Gilheany, D. G. Chromium and Manganese-salen Promoted Epoxidation of Alkenes. *Chem. Rev.* **2005**, *105*, 1563−1602.
(3) Mullins, C. S.; Pecoraro, V. L. Reflections on Small Molecule Manganese Models that Seek to Mimic Photosynthetic Water Oxidation Chemistry. *Coord. Chem. Rev.* **2008**, *252*, 416−443 The Role of Manganese in Photosystem {II}.
(4) Freire, C.; Pereira, C.; Rebelo, S. *Catalysis: Vol. 24*; The Royal Society of Chemistry, 2012; Vol. *24*; pp 116−203.
(5) Corma, A.; García, H.; Llabrés i Xamena, F. X. Engineering Metal Organic Frameworks for Heterogeneous Catalysis. *Chem. Rev.* **2010**, *110*, 4606−4655.
(6) Khavrutskii, I. V.; Musaev, D. G.; Morokuma, K. Epoxidation of Unfunctionalized Olefins by Mn(salen) Catalyst Using Organic Peracids as Oxygen Source: A Theoretical Study. *Proc. Natl. Acad. Sci. U.S.A.* **2004**, *101*, 5743−5748.
(7) Kürti, L.; Blewett, M. M.; Corey, E. J. Origin of Enantioselectivity in the Jacobsen Epoxidation of Olefins. *Org. Lett.* **2009**, *11*, 4592−4595.
(8) Adam, W.; Roschmann, K. J.; Saha-Möller, C. R. A Novel Counterion Effect on the Diastereoselectivity in the MnIII(salen)-Catalyzed Epoxidation of Phenyl-Substituted cis-Alkenes. *Eur. J. Org. Chem.* **2000**, *2000*, 3519−3521.
(9) Abashkin, Y. G.; Collins, J. R.; Burt, S. K. (Salen)Mn(III)-Catalyzed Epoxidation Reaction as a Multichannel Process with Different Spin States. Electronic Tuning of Asymmetric Catalysis: A Theoretical Study. *Inorg. Chem.* **2001**, *40*, 4040−4048.
(10) Cavallo, L.; Jacobsen, H. Electronic Effects in (salen)Mn-Based Epoxidation Catalysts. *J. Org. Chem.* **2003**, *68*, 6202−6207.
(11) Cavallo, L.; Jacobsen, H. Toward a Catalytic Cycle for the Mn−Salen Mediated Alkene Epoxidation: A Computational Approach. *Inorg. Chem.* **2004**, *43*, 2175−2182.
(12) Jacobsen, H.; Cavallo, L. Donor-Ligand Effect on the Product Distribution in the Manganese-Catalyzed Epoxidation of Olefins: A Computational Assessment. *Organometalics* **2006**, *25*, 177−183.
(13) Malek, K.; Li, C.; van Santen, R. A. New Theoretical Insights Into Epoxidation of Alkenes by Immobilized Mn−salen Complexes in

Mesopores: Effects of Substrate, Linker and Confinement. *J. Mol. Catal. A: Chem.* **2007**, *271*, 98−104.
(14) Teixeira, F.; Mosquera, R. A.; Melo, A.; Freire, C.; Cordeiro, M. N. D. S. Principal Component Analysis of Mn(salen) Catalysts. *Phys. Chem. Chem. Phys.* **2014**, DOI: 10.1039/c4cp00721b.
(15) Campbell, K. A.; Lashley, M. R.; Wyatt, J. K.; Nantz, M. H.; Britt, R. D. Dual-Mode EPR Study of Mn(III) Salen and the Mn(III) Salen-Catalyzed Epoxidation of *cis*-*β*-Methylstyrene. *J. Am. Chem. Soc.* **2001**, *123*, 5710−5719 PMID: 11403603.
(16) Kurahashi, T.; Kikuchi, A.; Shiro, Y.; Hada, M.; Fujii, H. Unique Properties and Reactivity of High-Valent Manganese−Oxo versus Manganese−Hydroxo in the Salen Platform. *Inorg. Chem.* **2010**, *49*, 6664−6672.
(17) Abashkin, Y. G.; Burt, S. K. (salen)MnIII Compounds as Nonpeptidyl Mimics of Catalase. Mechanism-Based Tuning of Catalase Activity: A Theoretical Study. *Inorg. Chem.* **2005**, *44*, 1425−1432.
(18) Abashkin, Y. G.; Burt, S. K. (Salen)Mn-Catalyzed Epoxidation of Alkenes: A Two-Zone Process with Different Spin-State Channels as Suggested by DFT Study. *Org. Lett.* **2004**, *6*, 59−62.
(19) Adam, W.; Stegmann, V. R.; Saha-Möller, C. R. Regio- and Diastereoselective Epoxidation of Chiral Allylic Alcohols Catalyzed by Manganese(salen) and Iron(porphyrin) Complexes. *J. Am. Chem. Soc.* **1999**, *121*, 1879−1882.
(20) Biswas, A. N.; Das, P.; Kandar, S. K.; Agarwala, A.; Bandyopadhyay, D.; Bandyopadhyay, P. Chiral Mn(III) Salen Catalyzed Oxidation of Hydrocarbons. *Trans. Met. Chem.* **2010**, *35*, 527−530.
(21) Gascon, J.; Corma, A.; Kapteijn, F.; Llabrés i Xamena, F. X. Metal Organic Framework Catalysis: Quo Vadis? *ACS Catal.* **2014**, *4*, 361−378.
(22) Gaspar, H.; Andrade, M.; Pereira, C.; Pereira, A. M.; Rebelo, S. L. H.; Araujo, J. P.; Pires, J.; Carvalho, A. P.; Freire, C. Alkene Epoxidation by Manganese(III) Complexes Immobilized Onto Nanostructured Carbon CMK-3. *Catal. Today* **2013**, *203*, 103−110.
(23) Ma, L.; Su, F.; Guo, W.; Zhang, S.; Guo, Y.; Hu, J. Epoxidation of Styrene Catalyzed by Mesoporous Propylthiol Group-Functionalized Silica Supported Manganese(III) Salen Complexes with Different Pore Morphologies. *Microporous Mesoporous Mater.* **2013**, *169*, 16−24.
(24) Maia, F.; Silva, R.; Jarrais, B.; Silva, A. R.; Freire, C.; Pereira, M. F. R.; Figueiredo, J. L. Pore Tuned Activated Carbons as Supports for an Enantioselective Molecular Catalyst. *J. Colloid Interface Sci.* **2008**, *328*, 314−323.
(25) Kuzniarska-Biernacka, I.; Silva, A. R.; Carvalho, A. P.; Pires, J.; Freire, C. Direct Immobilisation Versus Covalent Attachment of a Mn(III)salen Complex Onto an Al-Pillared Clay and Influence in the Catalytic Epoxidation of Styrene. *J. Mol. Catal. A: Chem.* **2007**, *278*, 82−91.
(26) Mahata, N.; Silva, A. R.; Freire, C.; Castro, B. D.; Figueiredo, J. L. Anchoring of a [Mn(salen)Cl] Complex onto Mesoporous Carbon Xerogels. *J. Colloid Interface Sci.* **2007**, *311*, 152−158.
(27) Das, P.; Kuzniarska-Biernacka, I.; Silva, A. R.; Carvalho, A. P.; Pires, J.; Freire, C. Encapsulation of Chiral Mn(III) Salen Complexes Into Aluminium Pillared Clays: Application as Heterogeneous Catalysts in the Epoxidation of Styrene. *J. Mol. Catal. A: Chem.* **2006**, *248*, 135−143.
(28) Silva, A. R.; Wilson, K.; Clark, J. H.; Freire, C. Covalent Attachment of Chiral Manganese(III) Salen Complexes onto Functionalised Hexagonal Mesoporous Silica and Application to the Asymmetric Epoxidation of Alkenes. *Microporous Mesoporous Mater.* **2006**, *91*, 128−138.
(29) Silva, A. R.; Vital, J.; Figueiredo, J. L.; Freire, C.; Castro, B. D. Activated Carbons with Immobilised Manganese(III) Salen Complexes as Heterogeneous Catalysts in the Epoxidation of Olefins: Influence of Support and Ligand Functionalisation on Selectivity and Reusability. *New J. Chem.* **2003**, *27*, 1511−1517.
(30) Jensen, F. *Introduction to Computational Chemistry*, 2nd ed.; John Wiley & Sons Ltd: Chichester, England, 2007.
(31) Neese, F. Prediction of Molecular Properties and Molecular Spectroscopy with Density Functional Theory: From Fundamental Theory to Exchange-coupling. *Coord. Chem. Rev.* **2009**, *253*, 526−563.
(32) Cortés-Guzmán, F.; Bader, R. F. W. Complementarity of QTAIM and MO Theory in the Study of Bonding in Donor-acceptor Complexes. *Coord. Chem. Rev.* **2005**, *249*, 633−662.
(33) Martin, F.; Zipse, H. Charge Distribution in the Water Molecule—A Comparison of Methods. *J. Comput. Chem.* **2005**, *26*, 97−105.
(34) Teixeira, F.; Mosquera, R. A.; Melo, A.; Freire, C.; Cordeiro, M. N. D. S. Charge Distribution in Mn(salen) Complexes. *Int. J. Quantum Chem.* **2014**, *114*, 525−533.
(35) Bader, R. F. W. *Atoms in Molecules: A Quantum Theory*; Oxford University Press: New York, 1990.
(36) Xiang, S.; Zhang, Y.; Xin, Q.; Li, C. Enantioselective Epoxidation of Olefins Catalyzed by Mn(salen)/MCM-41 Synthesized With a New Anchoring Method. *Chem. Commun.* **2002**, *2002*, 2696−2697.
(37) Zhang, H.; Xiang, S.; Li, C. Enantioselective Epoxidation of Unfunctionalised Olefins Catalyzed by Mn(salen) Complexes Immobilized in Porous Materials via Phenyl Sulfonic Group. *Chem. Commun.* **2005**, *2005*, 1209−1211.
(38) Das, P.; Silva, A. R.; Carvalho, A. P.; Pires, J.; Freire, C. Enantioselective Epoxidation of Alkenes by Jacobsen Catalyst Anchored onto Aminopropyl-functionalised Laponite, MCM-41 and FSM-16. *Catal. Lett.* **2009**, *129*, 367−375.
(39) Jacobsen, H.; Cavallo, L. Re-evaluation of the Mn(salen) Mediated Epoxidation of Alkenes by Means of the B3LYP* Density Functional. *Phys. Chem. Chem. Phys.* **2004**, *6*, 3747−3753.
(40) Neese, F. The ORCA Program System. *WIREs Comput. Mol. Sci.* **2012**, *2*, 73−78.
(41) Xu, X.; Goddard, W. A., III The X3LYP Extended Density Functional for Accurate Descriptions of Nonbond Interactions, Spin States, and Thermochemical Properties. *Proc. Natl. Acad. Sci. U.S.A.* **2004**, *101*, 2673−2677.
(42) Xu, X.; Zhang, Q.; Muller, R. P.; Goddard, W. A., III An Extended Hybrid Density Functional (X3LYP) with Improved Descriptions of Nonbond Interactions and Thermodynamic Properties of Molecular Systems. *J. Chem. Phys.* **2005**, *122*, 014105.
(43) Schaefer, A.; Horn, H.; Ahlrichs, R. Fully Optimized Contracted Gaussian Basis Sets for Atoms Li to Kr. *J. Chem. Phys.* **1992**, *97*, 2571−2577.
(44) The Ahlrichs (2d,2p) polarization functions were obtained from the TurboMole basis set library. ftp.chemie.uni-karlsruhe.de/pub/basen (retrieved 25/09/2012).
(45) Cavallo, L.; Jacobsen, H. Manganese-Salen Complexes as Oxygen-Transfer Agents in Catalytic Epoxidations—A Density Functional Study of Mechanistic Aspects. *Eur. J. Inorg. Chem.* **2003**, *2003*, 892−902.
(46) Zou, W. Molden2AIM, version 2.0.6. http://people.smu.edu/wzou/program/index.html (retrieved 01/11/2012).
(47) Keith, T. A. AIMAll (Version 13.11.04). 2013; http://aim.tkgristmill.com/ (retrieved 05/03/2013).
(48) Bader, R. F. W. AIMPAC: *A suite of programs for the AIM theory*. www.chemistry.mcmaster.ca/aimpac, Retrieved from: https://github.com/ecbrown/aimpac (01/10/2012).
(49) Matta, C. F.; Boyd, R. J. In *The Quantum Theory of Atoms in Molecules: From Solid State to DNA and Drug Design*; Matta, C. F., Boyd, R. J., Eds.; Wiley-VCH: Weinheim, 2007; pp 1−30.
(50) R Core Team, R: *A Language and Environment for Statistical Computing*. R Foundation for Statistical Computing: Vienna, Austria, 2013.
(51) Krzystek, J.; Telser, J. High Frequency and Field EPR Spectroscopy of Mn(III) Complexes in Frozen Solutions. *J. Magn. Reson.* **2003**, *162*, 454−465.
(52) Bryliakov, K. P.; Babushkin, D. E.; Talsi, E. P. Detection of {EPR} Spectra in *S* = 2 States of MnIII(salen) Complexes. *Mendeleev Commun.* **1999**, *9*, 29−31.

(53) Sears, J. S.; Sherrill, C. D. The Electronic Structure of oxo-Mn(salen): Single-reference and Multireference Approaches. *J. Chem. Phys.* **2006**, *124*, 144314.
(54) Malek, K.; Jansen, A. P. J.; Li, C.; van Santen, R. A. Enantioselectivity of Immobilized Mn-salen Complexes: A Computational Study. *J. Catal.* **2007**, *246*, 127−135.
(55) Estévez, L.; Mosquera, R. A. Where is the Positive Charge of Flavylium Cations? *Chem. Phys. Lett.* **2008**, *451*, 121−126.
(56) Stutchbury, N. C. J.; Cooper, D. L. Charge Partitioning by Zero-Flux Surfaces: The Acidities and Basicities of Simple Aliphatic Alcohols and Amines. *J. Chem. Phys.* **1983**, *79*, 4967−4972.